

**THE IMPORTANCE OF POSITIONING ISOLATED NEUTRON STARS:  
THE CASE OF GEMINGA**

**P.A. Caraveo<sup>1</sup>, M.G. Lattanzi<sup>2</sup>, G. Massone<sup>2</sup>, R. Mignani<sup>3</sup>, V.V. Makarov<sup>4</sup>,  
M.A.C. Perryman<sup>5</sup>, G.F. Bignami<sup>6,1</sup>**

<sup>1</sup>Istituto di Fisica Cosmica del CNR, Via Bassini, 15, 20133 Milano, Italy

<sup>2</sup>Osservatorio Astronomico di Torino, 10025 Pino Torinese, Italy

<sup>3</sup>Max-Planck-Institute für Extraterrestrische Physik, Garching, Germany

<sup>4</sup>Copenhagen University Observatory, 1350 Copenhagen K, Denmark

<sup>5</sup>Astrophysics Division, ESTEC, 2200AG Noordwijk, The Netherlands

<sup>6</sup>Agenzia Spaziale Italiana, Via di Villa Patrizi 13, Roma, Italy

ABSTRACT

We report on a multi-step procedure aimed at measuring, with high accuracy, the coordinates of Geminga within the Hipparcos and Tycho systems. Starting with an astrometric plate containing few tens of Tycho stars and 4 Hipparcos ones, we went through four intermediate steps to measure, to about 0.040 arcsec (per coordinate), the absolute position of Geminga in an HST Planetary Camera image. This positional accuracy, unprecedented for the optical position of an object this faint, is slightly better than that of the Crab pulsar, a comparable source of high energy  $\gamma$ -rays but about 9 magnitudes brighter in the visible. This result, made possible by the availability of both Hipparcos and HST data, will allow significant refinement on the timing parameters of this source of copious  $\gamma$ -ray emission.

Key words: space astrometry; pulsar; Geminga.

1. INTRODUCTION

To properly analyze the timing signature of a rapidly varying source, such as a pulsar, the photon arrival times must be corrected for the motion of the detector, be it on the ground or onboard a satellite. Arrival times are corrected for the light travel time they would have needed to reach the barycentre of the solar system and the procedure, routinely applied before any time analysis at any wavelength, is called barycentricization. Such a correction is maximum for sources located near to the ecliptic plane while its magnitude decreases for sources at high ecliptic latitude. Any error on the source coordinates would affect the accuracy of the corrected arrival times and thus limit the precision potentially achievable for the measure of the source timing parameters.

Indeed, the position of a radio pulsar is obtained by minimizing its timing residuals over a reasonably long

time span. However, a number of factors, such as the pulsar period (fast pulsars are positioned with higher accuracy than slow ones), timing noise and glitching activity, come into play to limit the positional accuracy achievable with radio data.

Precise optical positioning of pulsar counterparts can give a significant contribution to improve the accuracy of the timing analysis and to reduce uncertainties in the determination of the pulsar  $\nu$  and  $\dot{\nu}$ . This is a crucial step to nail down the pulsar frequency second derivative, aiming at the measurement of its braking index  $n = \ddot{\nu}/\dot{\nu}^2$ . This quantity, expected to be 3 for magnetic dipole braking, has been measured so far for young objects such as Crab (Lyne et al. 1988), PSR 0540-69 (Guiffes et al. 1992), PSR 1509-58 (Kaspi et al. 1994), and PSR 0833-45 (Lyne et al. 1996). Table 1 lists the pulsar parameters relevant for the braking index measurement, namely: the value of period and its derivative, the accuracy achieved in the measure of such derivative as well as on the objects' coordinates, the characteristic age, the frequency second derivative and the braking index itself. Table 1 also shows the importance of accurate optical positioning for the determination the timing parameters of pulsars affected by significant timing noise, such as the Crab and Vela pulsars, or too faint to be accurately positioned in radio, such as PSR 0540-69. Indeed, the only object relying on radio coordinates is PSR 1509-58, the optical identification of which is tentative (Caraveo et al. 1994).

Optical positioning is all the more important for Geminga, so far a unique example of radio quiet neutron star (Caraveo et al. 1996b) The radio silence of the source makes it impossible to access the information on its position and distance as inferred from the optimization of the radio timing parameters and from the dispersion measure of the radio pulses. Thus, to measure position, distance and timing parameters of Geminga all other branches of astronomy had to be exploited in a 20-year long chase, recently summarized by Bignami & Caraveo (1996).

Briefly, the source was discovered in high energy  $\gamma$ -ray by the SAS-2 satellite in 1972 (Fichtel et al.

Table 1. Pulsars with measured braking index  $n = v\ddot{v}/\dot{v}^2$ .

Name	$P$ (s)	$\dot{P}$ (s/s)	$\Delta P$ (s/s)	$\Delta\alpha$ (sec)	$\Delta\delta$ (arcsec)	Age (y)	$n$	$\dot{v}$
PSR0531+21	0.033	$4.2 \cdot 10^{-13}$	$2 \cdot 10^{-19}$	0.005	$0.06^{(1)}$	1,260	$2.5 \pm 0.01$	$1.2 \cdot 10^{-20}$
PSR1509-58	0.151	$1.5 \cdot 10^{-12}$	$1 \cdot 10^{-19}$	0.089	1	1,545	$2.8 \pm 0.01$	$1.9 \cdot 10^{-21}$
PSR0540-69	0.050	$4.8 \cdot 10^{-13}$	$8 \cdot 10^{-19}$	0.029	$0.49^{(2)}$	1,670	$2.0 \pm 0.2$	$3.7 \cdot 10^{-21}$
PSR0833-45	0.089	$1.2 \cdot 10^{-13}$	$2 \cdot 10^{-17}$	0.019	$0.29^{(3)}$	11,350	$1.6 \pm 0.3$	$3.5 \cdot 10^{-23}$
Geminga	0.237	$1.1 \cdot 10^{-14}$	$1.4 \cdot 10^{-19}$	$0.003^{(4)}$	$0.040^{(4)}$	$3.5 \cdot 10^5$	??	??

<sup>(1)</sup> McNamara 1971

<sup>(2)</sup> Caraveo et al., 1992, ApJ Lett. 395, L103

<sup>(3)</sup> Manchester et al. 1978

<sup>(4)</sup> present work

1975), an X-ray counterpart, suggesting position and distance, has been proposed in 1983 (Bignami et al. 1983) and an optical one, refining the position, in 1987/88 (Bignami et al. 1987, Halpern & Tytler 1988). However, the breakthrough came with the discovery of the 237 ms periodicity in the ROSAT data (Halpern & Holt 1992). Finding the same periodicity in the simultaneous high energy  $\gamma$ -ray data of the EGRET instrument (Bertsch et al. 1992), as well as in the old archival COS-B (Bignami & Caraveo 1992) and SAS-2 data (Mattox et al. 1992), yielded the value of the period derivative and thus of the object's energetics. The discovery of the proper motion of the proposed optical counterpart (Bignami et al. 1993) confirmed the optical identification and, thus, provided the absolute positioning of Geminga to within 1 arcsec, i.e. the systematic uncertainty of the Guide Star Catalogue (Taff et al. 1990). Next came the measure of the source parallactic displacement, yielding a precise measure of its distance (Caraveo et al. 1996a).

Our knowledge of the Geminga pulsar is now good enough to warrant, 'honoris causa', inclusion in the radio pulsar catalogue of Taylor et al. (1993). Indeed, the radio silent Geminga stands out among normally behaving radio pulsars for the remarkable accuracy achieved in the measure of its parameters. Inspection of the pulsar catalogue shows that the period derivative of Geminga is known with an accuracy greater than that of the Crab (see Table 1). This is mainly due to the very stable behaviour of this  $10^5$  y old neutron star which does not seem to be affected by the glitching activity typical of younger objects, nor by significant timing noise. Indeed, Mattox et al. (1996) claim that, during the first 3 years of EGRET coverage, every pulsar revolution can be accounted for. Thus, the  $\gamma$ -ray photons, collected in week-long observing periods taken several month apart over a span of years, can be aligned in phase to form the very spiky light curve seen in high energy  $\gamma$ -rays.

Had Geminga have been a glitching pulsar like Vela or Crab, it would have been impossible to obtain a satisfactory (and accurate) long-term solution. Indeed, the growing high energy coverage offers the possibility to further exploit the stability of Geminga to refine the knowledge of the source timing parameters, including the second period derivative and, thus, the source braking index. However, to take full advantage of the potentialities offered by  $\gamma$ -ray astronomy, a very accurate value of the source absolute coordinates is required to barycenterize the arrival time of each photon. This procedure is particularly critical

for Geminga, which is located very near the ecliptic equator, where the barycentric correction is maximum. Mattox et al. (1996) have shown that the uncertainty in the source absolute positioning can induce an error in the barycentric correction up to  $2.3 \delta_e$  ms, where  $\delta_e$  is the source positional uncertainty (in arcsec) projected on the plane of the ecliptic. Thus, with a sensitivity to phase errors of  $10^{-2}$  over a period of 237 ms, the positional accuracy of 1 arcsec presently available is the limiting factor for Geminga's photon timing analysis.

A one order of magnitude better absolute position is mandatory to phase together SAS-2, COS-B and EGRET data. However, to measure the absolute position Geminga, one has to overcome the severe magnitude gap between the bright stars used as primary reference and the  $m_v = 25.5$  target.

This was accomplished with a program of dedicated astrometric measurements carried out at the Torino Observatory which, in conjunction with Hipparcos and HST data, yielded for Geminga a position of unprecedented accuracy.

## 2. ABSOLUTE ASTROMETRY

The best optical reference frame on the sky is now that provided by the Hipparcos and Tycho Catalogues (ESA 1997). While the Hipparcos Catalogue lists 118 000 stars as faint as  $V = 12.4$  mag whose positions and annual proper motions are known to typically 1 mas at epoch J1991.25, the Tycho Catalogue contains more than one million objects, the astrometric parameters of which have been measured with a median accuracy of 25 mas. With about 3 stars per square degree the Hipparcos Catalogue, although of vastly superior accuracy, is not suitable for our purpose, which can be better fulfilled by the relatively less accurate but denser Tycho Catalogue. However, since the proper motions listed in the Tycho Catalogue are accurate only to approximately 25 mas/yr, we have propagated the Tycho positions to the appropriate plate epochs using the proper motions provided by the PPM catalogue (Rösner & Bastian 1993). This all-sky list of 378 910 stars referred to the FK5 system provides proper motions with a typical accuracy of 4 mas/yr. Consequently, we shall be using a subset of the Tycho objects also listed in the PPM catalogue as our primary reference.

Unfortunately, none of the presently available com-

binations of telescope and detector is able to cover the gap of  $\sim 16$ -18 magnitudes between the rather bright Tycho/PPM stars and Geminga. In order to cover this large dynamical range, we had to break down the link into several steps.

The principle of the method is to cover the field of interest with images of increasingly smaller field of view and deeper limiting magnitude. The transfer of the reference system from one step to the next is based on a set of stars of intermediate magnitude. In general, the following considerations applies:

- (a) the useful dynamical range of a typical astronomical detector is of the order of 5 magnitudes, to avoid saturation problems at the bright end and exceedingly low s/n ratio for the faintest stars to be measured;
- (b) for the first step, the field of view must cover a region on the sky big enough to contain an adequate number of reference stars from the selected primary catalogue;
- (c) the unavoidable errors introduced in the process of transferring the reference system through sets of intermediate reference stars must be kept as small as possible.

A similar procedure has been successfully applied by, e.g. Chiumento et al. (1991) and Zacharias et al. (1995) for the determination of absolute positions of optical counterparts of extragalactic radio-sources. However, these cases were less critical, as the difference in magnitude was only 8–10 and two or three intermediate steps were usually sufficient to bridge the gap between the reference stars and the targets.

We note in passing that the FK4 coordinates of the 16 mag Crab pulsar, were obtained by McNamara (1971) with a two step procedure.

In the case of Geminga ( $V=25.5$  mag), we had to use a five-step procedure which starts with astrometric plates taken at Torino Observatory (OATo), and ends with images taken with the Planetary Camera 2 on HST. The observational material used in this study is listed in Table 2.

The procedure starts with the calibration of the images taken with the 38 cm photographic refractor at Pino Torinese Observatory. On these plates, 19 Tycho stars, also listed in the PPM catalogue, define the primary reference while a grid of 17 fainter stars is used as the secondary reference frame. This grid of fainter stars acts as the ‘primary reference frame’ on the plates taken with the 105 cm astrometric reflector (step 2). The procedure is then repeated for the following steps, ending with a grid of reference stars suitable for the astrometric calibration of the WFPC2 frame (see Figure 1).

### 3. ERROR ANALYSIS

The final error on the coordinates of Geminga, as obtained through our five-step procedure, is due to the combination of three components. The first one,

Table 3. Centering ( $\epsilon_r$ ) and transformation ( $\epsilon_{tr}$ ) errors at each astrometric reduction step. The last two values (step 5) are educated guesses and not direct estimates, as for the other data. See text for detailed explanations.

Step	$\epsilon_r$	$\epsilon_{tr}$
1	0 <sup>o</sup> .102	0 <sup>o</sup> .044
2	0 .061	0 .020
3	0 .026	0 .011
4	0 .015	0 .008
5	[0 .005]	[0 .003]

$\epsilon_{\text{Tycho}}$ , measures the precision with which we can register the secondary reference frame on the refractor images, the second,  $\epsilon_r$ , random in nature, is basically the image centering error, while the third,  $\epsilon_{\text{sys}}$ , is systematic and results from the least-square adjustments,  $\epsilon_{tr}$ , used, at each step, to generate the lists of secondary stellar grids (Eichhorn 1974). Table 3 summarizes the centering errors  $\epsilon_r$  and the systematic ones  $\epsilon_{tr}$  for each step of our procedure. The  $\epsilon_r$ 's were evaluated using the formula  $\sigma_r(i) \sim \sigma_0(i+1)$ , i.e. the random error at step  $i$  is taken as the mean error of unit weight at step  $i+1$ . This assumes that, after step 1 (at which the error of the reference catalogue must be taken into account), the mean error of unit weight of each least squares adjustment at step  $i+1$  (one per coordinate) is close to the measuring error at step  $i$ . The values in Table 3 are indeed consistent with our measuring practice of similar plate material; centering errors are typically  $\sim 1.0$ – $1.5 \mu\text{m}$  per rectangular coordinate for well exposed stellar images, and a factor of 1.5–2 worse for images 1 mag above the plate limit, as it is typically the case for stars defining the secondary reference frames on the refractor plates. Following Lattanzi et al. (1997), the systematic error at each step, i.e. the error of the transformation, can be written as  $\epsilon_{tr} \sim \sqrt{3} \times \epsilon_r / \sqrt{m}$ , where  $\epsilon_r$  is the average measuring error of the stars in the primary reference catalogue at that particular step, 3 is the number of free parameters in the linear plate-to-field transformations used, and  $m$  is the number of reference stars. Of course, unknown proper motions of the reference stars used to calibrate frames taken at different epochs (as for the images from the astrometric reflector, SUSI and the PC2) are included in the values of  $\epsilon_r$  and  $\epsilon_{tr}$  quoted in Table 3.

We note that, for steps 3 and 4, the combinations of telescope scale and image sampling are so favourable that centering errors (even for the faintest secondary stars) are small. This is also true for the WFPC2 solution (step 5); for which the centering error is conservatively taken to be 0.005 arcsec ( $\sim 1/10$  pixel) both for Geminga and for the (better exposed) objects defining the local frame of reference.

The step-by-step errors, given in Table 3, are the starting point to compute the astrometric error on Geminga's position. Since we have to estimate the precision of the ‘positioning’ of Geminga within the Tycho/Hipparcos frame, it is necessary to evaluate first the error of the position of our object relative to each local frame (one per step). Thus, the *random* contribution to the final error is *simply* the centering error of our target relative to reference stars on the WFPC-2 frame., i.e.  $\epsilon_r = 0.005$  arcsec. To this,

Table 2. The stars in the secondary grid of step  $n$  (4th column) become the primary grid of step  $n + 1$  (3rd column). Since some of the secondary grid stars measured at step  $n$  could not be satisfactorily measured on the image of step  $n+1$  (owing to, for example, saturation, duplicity, etc.) the numbers in the two columns can be different. The last column lists the number of plates/frames available for each telescope/detector combination.

telescope/detector	field of view [epoch]	primary grid	secondary grid	images [steps]
OATo 38cm refractor plate, 30"/mm	70' x 70' [1984.19]	19 Tycho/PPM	17	2 [1 and 1bis]
OATo 105cm reflector plate, 20".7/mm	30' x 30' [1984.19]	16	28	2 [2 and 2bis]
OATo 105cm reflector CCD, 0".48/px	9' x 10' [1996.13]	26	21	2 [3 and 3bis]
ESO NTT 3.5m, SUSI CCD 0".13/px	2.5' x 2.5' [1992.86]	16	10	1 [4]
HST 2.4m, PC2 CCD, 0".046/px	35" x 35" [1995.21]	10	Geminga	1 [5]

we have to add, in quadrature, the systematic component  $\epsilon_{\text{sys}} = \simeq 0.050$  arcsec, obtained by adding in quadrature the plate-to-plate transformations  $\epsilon_{\text{tr}}$  listed in Table 3.

The value of  $\sqrt{\epsilon_{\text{r}}^2 + \epsilon_{\text{sys}}^2}$  represents the precision of the positioning of Geminga within the reference frame defined by the secondary reference stars on the refractor plate. To this error we have to add, again in quadrature, the error of the registration of such secondary frame relative to that defined by the nineteen Tycho/PPM stars used as primary references, i.e.  $\epsilon_{\text{Tycho}} \sim \sqrt{3} \times \sigma_{\text{Tycho}} / \sqrt{19}$ , where  $\sigma_{\text{Tycho}} \simeq 0.032$  arcsec is the mean error (per coordinate) at the epoch of the refractor plate accounting for both the average errors in the Tycho positions (in our case 15 mas) and the uncertainty on PPM proper motions propagated over 7 years. Therefore, the error (per coordinate) on a single-solution position of Geminga in the Hipparcos system is:

$$\sqrt{\epsilon_{\text{Tycho}}^2 + \epsilon_{\text{r}}^2 + \epsilon_{\text{sys}}^2} \sim 0.052 \text{ arcsec}$$

Since, as stated in Table 2, we have two images for steps 1 through 3, we have repeated the measurements of the stars selected as primary and secondary grids and we have used the mean of the two independent measures. This has the advantage to reduce the systematic error by a factor  $\sqrt{2}$  so that the error (per coordinate) of the averaged position is  $\sqrt{\epsilon_{\text{Tycho}}^2 + 1/2 \epsilon_{\text{sys}}^2 + \epsilon_{\text{r}}^2} \simeq 0.040$  arcsec, where the  $1/\sqrt{2}$  factor has been applied only to the  $\epsilon_{\text{sys}}$ , since  $\epsilon_{\text{Tycho}}$  and  $\epsilon_{\text{r}}$  are the same for both solutions.

### 3.1. Geminga's absolute position

The position of Geminga, determined within the Hipparcos reference frame and therefore connected directly to the ICRS, is (epoch 1995.21):

$$\alpha = 6^{\text{h}} 33^{\text{m}} 54.1530^{\text{s}}, \delta = 17^{\circ} 46' 12.909''$$

with a standard error in each coordinate of 40 mas.

As a consistency check, we have repeated the whole procedure using the four Hipparcos stars present in our first astrometric frame. Unfortunately, two of the four stars are pretty close so that only three positions are actually constraining the solution which is practically degenerate from the least-square point of view. Therefore no formal error is available on the Hipparcos position which turns out to be:

$$\alpha = 6^{\text{h}} 33^{\text{m}} 54.1477^{\text{s}}, \delta = 17^{\circ} 46' 12.945''$$

with an error certainly not smaller than the Tycho one. We note that the difference between the Tycho and Hipparcos positions is fully consistent with the errors quoted above.

## 4. CONCLUSIONS

The combination of ground based astrometric images, Hipparcos and Tycho catalogues and HST high resolution frames have provided us with a position of Geminga whose accuracy is unprecedented for an object this faint. The improvement on the accuracy of the source absolute position is more than one order of magnitude. Among the pulsars seen as high energy emitters, Geminga's positional accuracy is the best so far, better than that of the 9-mag brighter Crab pulsar. This improved position, in conjunction with the HST measure of the proper motion (Caraveo et al. 1996a), will allow the accurate barycentricization of all the  $\gamma$ -ray data collected so far.

It will thus be possible to measure the source second derivative and, hence, its braking index.

While the results obtained for the three young objects (see Table 1) are not too far from the canonical value of 3, the braking index recently measured for the older Vela pulsar is definitely lower.

Hence, the importance to take advantage of the stability of the  $10^5$  y old Geminga to considerably enlarge the pulsar age sampled for braking index determination. The task is a challenging one: for a braking index of 3, a  $\ddot{\nu}$  of  $2.7 \cdot 10^{-26} \text{ s}^{-3}$  is expected. This value is three order of magnitude smaller than that recently measured for Vela and 6 order of magnitude

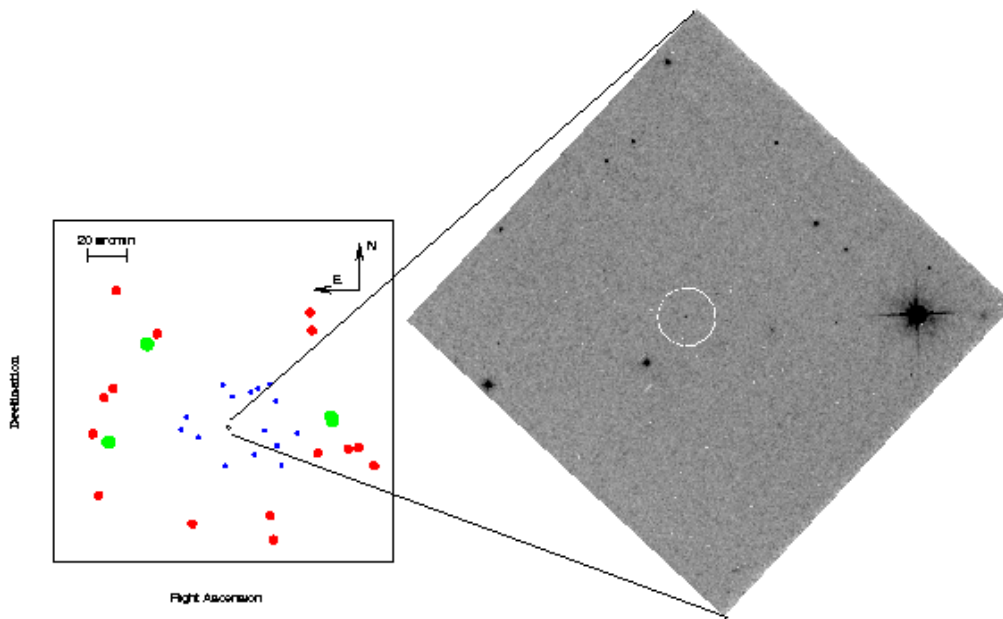


Figure 1. Comparison between the first and the last step of our procedure. Left: schematic representation of the  $70 \times 70 \text{ arcmin}^2$  astrometric plate taken at the OATo. Hipparcos stars are marked with large filled circles, Tycho stars with medium circles, while the small circles in the central region of the plate identify the stars used as secondary reference frame. The diamond in the center gives the position and actual dimension of the HST image, which represents the last step of our chain. Right:  $35 \times 35 \text{ arcsec}^2$  Planetary Camera image of the field of Geminga obtained with a 4400 sec exposure through filter 555, roughly equivalent to V. Geminga is shown inside a white circle.

smaller than that of the Crab. However, it appears to be within reach of the combined COS-B and EGRET data. Even a significantly smaller, Vela-like, braking index should be measurable.

What makes Geminga suitable for the measurement of such a tiny value of the frequency second derivative? If we order known pulsars according to increasing values of  $\ddot{\nu}$  (expected for a braking index of 3), Geminga does not come out prominently. Not less than 40 pulsars have hypothetical  $\ddot{\nu}$  bigger than the value expected for Geminga. However, for all of them, these values are not measurable because the errors on  $\nu$  and  $\dot{\nu}$  are too big. What singles out Geminga is the possibility to reduce such errors by phasing together 20 years worth of  $\gamma$ -ray data, now that the source positional accuracy is not a limiting factor. Thus, once again, Geminga appears to be in a special position amongst Isolated Neutron Stars. What matters most here is the source intrinsic stability, which made it worthwhile to devote a dedicated effort to the accurate measurement of its absolute position.

#### ACKNOWLEDGMENTS

We are grateful to the Hipparcos and Tycho collaborations who made the positions available to us prior to the official release of the catalogues.

#### REFERENCES

- Bertsch D.L., et al., 1992, *Nature*, 357, 306  
 Bignami, G.F., Caraveo, P.A., Lamb, R.C., 1983, *ApJ*, 272, L9  
 Bignami, G.F., Caraveo, P.A., Paul, J.A., Salotti, L., Vigroux, L., 1987, *ApJ*, 319, 358  
 Bignami, G.F., Caraveo, P.A. 1992, *Nature*, 357, 287  
 Bignami, G.F., Caraveo, P.A., Mereghetti, S., 1993, *Nature*, 361, 704  
 Bignami, G.F., Caraveo, P.A., Mignani, R., Edelstein, J., Bowyer, S. 1996, *ApJ*, 456, L111  
 Bignami, G.F., Caraveo, P.A., 1996, *ARA&A*, 34, 331  
 Caraveo, P.A., Bignami, G.F., Mignani, R., Taff, L.G., 1996a, *ApJ*, 461, L91  
 Caraveo, P.A., Bignami, G.F., Trümper, J.A., 1996, *Review A & A. Review*, 7, 209  
 Caraveo, P.A., Mereghetti, S., Bignami, G.F., 1994, *ApJ*, 423, L125  
 Caraveo, P.A., Bignami, G.F., Mereghetti, S., Mombelli, M., 1992, *ApJ*, 395, L103  
 Chiumento, G., Lattanzi, M.G., Massone, G., Morbidelli, I. R., Pannunzio, R., Sarasso, M., 1991, *A&A. Suppl.*, 184, 331  
 Eichhorn, H., 1974, *Astronomy of Star Positions*, Frederick Ungar Pu. Co., New York  
 ESA, 1997, *The Hipparcos and Tycho Catalogues*, ESA SP-1200  
 Halpern, J.H., Tytler, D., 1988, *ApJ*, 330, 201

- Halpern, J.P., Holt, S.S., 1992, *Nature*, 357, 222
- Fichtel, C.E., et al., 1975, *ApJ*, 198, 163
- Guiffes, C., Finley, J.P., Ögelman, H., 1992, *ApJ*, 394, 581
- Kaspi, V.M., Manchester, R.N., Siegman, B., Johnston, S., Lyne, A.G., 1994, *ApJ*, 422, L83
- Lattanzi, M.G., Capetti, A., Macchetto, F.D., 1997, *A&A*, 318, 997
- Lyne, A.G., Pritchard, R.S., Smith, F., 1988, *MNRAS*, 233, 667
- Lyne, A.G., Pritchard, R.S., Graham-Smith, F., Camilo, F., 1996, *Nature*, 381, 497
- Manchester, R.N., et al. 1978, *MNRAS*, 184, 159
- Mattox, J.R., Halpern, J.P., Caraveo, P.A., 1996, *A&A Suppl.*, 120C, 77
- Mattox, J.R. et al., 1992, *ApJ*, 103, 638
- McNamara, B.J. 1971, *PASP*, 83, 491
- Rösner, S., Bastian, U., 1993, *The Final PPM Star Catalogue for both Hemispheres*, *CDS Inf. Bull.*, 42, 11-16
- Taff, L.G., Lattanzi, M.G., Bucciarelli, B., Gilmozzi, R., McLean, B.J., Jenkner, H., Laidler, V.G., Lasker, B.M., Shara, M.M., Sturch, C.R., 1990, *ApJ*, 353, L45
- Taylor, J., Manchester, R.M., Lyne A.G., 1993, *ApJ Suppl.*, 88, 529
- Zacharias, N., De Vegt, C., Winter, L., Johnston, K. J., 1995, *AJ*, 110, 3093